

Research Article

Low Temperature Gasification of Coconut Shell with CO₂ and KOH: Effects of Temperature, Chemical Loading, and Introduced Carbonization Step on the Properties of Syngas and Porous Carbon Product

Natthaya Punsuwan,¹ Chaiyot Tangsathitkulchai,² and Takayuki Takarada³

¹Department of Chemical Engineering, Faculty of Engineering, Ubon Ratchathani University, Ubon Ratchathani 34190, Thailand

²School of Chemical Engineering, Institute of Engineering, Suranaree University of Technology, Nakhon Ratchasima 30000, Thailand

³Department of Chemical and Environmental Engineering, Gunma University, Kiryu 376-8515, Japan

Correspondence should be addressed to Chaiyot Tangsathitkulchai; chaiyot@sut.ac.th

Received 28 July 2015; Revised 26 October 2015; Accepted 26 October 2015

Academic Editor: Junwu Wang

Copyright © 2015 Natthaya Punsuwan et al. This is an open access article distributed under the Creative Commons Attribution License, which permits unrestricted use, distribution, and reproduction in any medium, provided the original work is properly cited.

Effect of KOH, reaction temperature and time, and introduced carbonization step on the amount and composition of syngas as well as porous properties of the carbon products for CO₂ gasification of coconut shell at low temperatures (300–700°C) was investigated. Results showed that the presence of potassium hydroxide and gasification temperature had a significant effect on the amount and composition of syngas product and facilitated the rate of hydrogen and carbon monoxide formation. It was also found that carbonization step could promote the generation of hydrogen gas as well as increasing the gas heating value per kg of gas. Furthermore, the porosity development of carbon product was found to be influenced by the chemical ratio and gasification temperature. The optimal conditions for achieving high hydrogen composition and specific surface area were to gasify coconut shell under CO₂ at 600°C for 60 min with carbonization step and with chemical weight ratio of 3.0. This condition gave the hydrogen composition as high as 29.70 %weight of produced syngas with heating value of 41.4 MJ/kg of gas and specific surface area of 2650 m²/g of the carbon product.

1. Introduction

The instability of price and supply of fossil fuels has necessitated the need for increasing utilization and development of alternative energy. Biomass is an attractive choice to substitute the conventional fossil fuels because of its abundant availability, its net zero emission of CO₂, and more importantly being renewable. There are a number of processes to convert biomass into energy such as fermentation, digestion, and thermal decomposition. The fermentation and digestion processes are relatively slow compared with thermal decomposition [1, 2]. Among biomass utilization technologies, thermal decomposition or thermochemical methods including combustion, pyrolysis, and gasification are thus currently the most appropriate and widely commercially

used. Gasification, a process that converts biomass at high temperatures (>700°C) under restricted amount of oxygen and in the presence of an external supply of oxidizing agents, such as pure oxygen, steam, and carbon dioxide, offers greater fuel flexibility because the syngas produced including methane, carbon monoxide, and hydrogen can be used either directly as fuel or as starting feedstocks for chemical production (e.g., methanol) or converted by the Fisher-Tropsch process into synthetic fuel. In addition, from the standpoint of combustion efficiency, gasification is superior to the direct combustion of original fuel since syngas can be combusted at a much higher temperature. The composition of the product gas, however, can vary significantly depending on the operating conditions [3], types of precursor [4], and types of gasifier [3, 4]. A gasification

process can be achieved in a variety of gasifiers: fixed bed gasifiers [5], fluidized bed gasifiers [6], and spouted bed gasifiers [7]. However, these technologies are always operable at a high temperature and pressure with the purpose to enhance the gasification performance [8]. Hence, in terms of energy utilization, it is better to operate a gasification system at a low temperature range and this can be realized by the application of an effective catalyst. García et al. (1999) [9] reported that the low temperature catalytic gasification process is a suitable and attractive choice to convert low-calorific value biomass waste into H_2 rich gas and to avoid the ash-related problems at high temperature such as sintering, agglomeration, decomposition, erosion, and corrosion. Various kinds of catalyst have been developed and tested for the gasification process. Several studies have shown that alkali metal salts, such as alkali carbonates [10], oxides, hydroxides and chlorides, and metal catalyst, such as nickel [11, 12], are effective catalysts in gasification. Earlier experiments showed that the usage of metal containing catalysts could accelerate the gasification rate [9, 13, 14], increase the gas yield, decrease the liquid and tar yields [2, 15, 16], and upgrade the fuel gas heating value by increasing hydrogen contents [15, 17]. Generally, the catalytic gasification is performed at relatively low temperatures ($<850^\circ C$) with a working temperature range depending on the type of precursors and catalysts used. Apart from the generated syngas product, the solid activated carbon product left from gasification can be further utilized as a sorbent material. However, the surface properties of an activated carbon from a gasification process will depend to a large extent on the preparation conditions and type of precursor materials.

With the purpose to lower energy consumption in a gasification process and to make use of abundantly available coconut shell in Thailand, it was decided in the present work to investigate the catalytic gasification of coconut shell biomass to simultaneously produce synthesis gas and a high porosity activated carbon at gasification temperatures lower than those encountered in normal practice. In this work, potassium hydroxide and carbon dioxide gas were employed as a catalyst and gasification oxidizing agent, respectively. Generally, potassium hydroxide is widely used as an activation agent since it can lead to optimal textural and chemical properties of the carbon [18], although the molecular details of activation mechanisms are not yet fully understood. Huang et al. (2009) [19] have reported the effects of metal catalysts on CO_2 gasification reactivity of biomass char. They found that the CO_2 gasification reactivity of char was improved via the addition of metal catalysts in the order of $K > Na > Fe > Mg$. Some previous works have also reported the enhanced production of hydrogen from catalytic steam gasification by employing potassium compounds [18, 20]. Furthermore, reports on the study of coconut shell gasification using both potassium hydroxide and carbon dioxide are quite limited. Therefore, the use of combined potassium hydroxide and carbon dioxide for the gasification of coconut shell to produce a high heat content gas fuel and a high porosity carbon adsorbent was the main objective of this work.

2. Experimental Section

2.1. Raw Material Characterization. Coconut shell was crushed by a jaw crusher and screened to obtain an average particle size of 1.55 mm (12×14 mesh). The sample obtained was then dried at $110^\circ C$ for 24 hours in an oven to remove excess moisture contained in the raw material and was kept for further analysis and experimentation. Chemical composition of coconut shell was determined by means of proximate and ultimate analyses. Proximate analysis was determined using a TGA analyzer (TGA 701, LECO) by following the analytical method ASTM D7582-12. Ultimate analysis was determined by using a CHNS analyzer (TruSpec CHN, LECO) to give elemental information on %weight of carbon, nitrogen, hydrogen, sulfur, and oxygen (by difference).

2.2. Coconut Shell Gasification. Coconut shell and potassium hydroxide were used, respectively, as a precursor and a catalyst for the gasification experiments. When the carbonization step was introduced prior to the gasification step, coconut shell precursor was heated in a muffle furnace under the atmosphere of flowing argon (100 mL/min) at $450^\circ C$ for 60 min using the heating rate of $10^\circ C/min$ and the final char yield was determined. The experimental procedure for the gasification study is as follows. Each of the precursors (raw coconut shell or coconut shell char from the carbonization step) of known weight was thoroughly mixed with potassium hydroxide powder according to the required catalyst to precursor weight ratio by keeping the total weight of mixture constant at 10 g. This solid mixture was then gasified in a fixed bed reactor made from a silica-alumina tube (45 mm ID and 600 mm in length) by heating at $10^\circ C/min$ from room temperature to the desired gasification temperature under a constant flow (100 mL/min) of oxidizing gas (50% Ar + 50% CO_2). The temperature and holding time for gasification were varied from 300 to $700^\circ C$ and from 30 to 180 min, respectively. During gasification, the produced gas products were passed through a water condenser to remove the liquid biooil and the remaining gas was continuously collected every 10 minutes in a 10-liter gas sampling bag until no gas products were generated which normally took about 240 min of gasification time. The main gas composition including CO, CO_2 , H_2 , CH_4 , and C_3H_8 in the product gases was determined by a gas chromatograph (Shimadzu, GC-2014) using a thermal conductivity detector (TCD) and flame ionization detector (FID), with helium gas being introduced as the carrier gas. The final solid product obtained was mixed with HCl solution (5% by volume concentration) and stirred for 1 hour, followed by rinsing with deionized water to remove any remaining potassium hydroxide and potassium hydroxide derivatives until the pH of the rinsing water was constant at proximately 7.0. Then, the carbon product was dried at $110^\circ C$ for 10–12 hours and weighed. Previous works have shown that HCl solution in the concentration range from 0.85 to 43% by volume has been employed to effectively remove contaminants from activated carbons produced by chemical activation with KOH [21–25].

The specific surface area of the activated carbon sample was determined from the N_2 adsorption isotherm at $77 K$

TABLE 1: Experimental conditions for studying low temperature catalytic gasification of coconut shell.

Sample code	Step I (carbonization)				Step II (gasification)			
	Temp. (°C)	HT (°C/min)	Time (min)	CR (g/g)	Temp. (°C)	HT (°C/min)	Time (min)	CO ₂ (%)
G01	—	—	—	0	600	10	180	50
G02	—	—	—	0.5	600	10	180	50
G03	—	—	—	0.75	600	10	180	50
G04	—	—	—	1.0	600	10	180	50
G05	—	—	—	1.5	600	10	180	50
G06	—	—	—	2.0	600	10	180	50
G07	—	—	—	0.75	300	10	180	50
G08	—	—	—	0.75	400	10	180	50
G09	—	—	—	0.75	500	10	180	50
G10	—	—	—	0.75	600	10	180	0*
G11	450	10	60	2.0	600	10	180	50
G12	450	10	60	2.0	600	10	60	50
G13	450	10	60	2.0	600	10	30	50
G14	450	10	60	3.0	600	10	60	50
G15	450	10	60	4.0	600	10	60	50
G16	450	10	60	4.0	700	10	60	50

* In the atmosphere of inert argon gas.

HT: heating rate.

CR: chemical-to-biomass weight ratio.

Time: holding time.

with an automatic sorption meter (BELSORP-max). The sample was placed into the sample tube, heated to 300°C, and evacuated until the pressure became less than 6.7×10^{-7} Pa prior to the surface area measurement. The Brunauer-Emmet-Teller (BET) theory [26] was used to determine the specific surface area of the activated carbon product. Total pore volume was calculated from the amount of N₂ gas adsorbed at a relative pressure of 0.95 and converted this amount to the volume of N₂ in liquid state. The t-plot method [26] was applied to calculate the micropore volume. The combined volume of mesopores and macropores was obtained by subtracting the micropore volume from the total pore volume.

X-ray diffraction (XRD) analysis of the activated carbon product was carried out by using a Shimadzu EDX-700 energy dispersive X-ray spectrometer with Cu K α radiation. XRD was performed on the powder samples ($d_p < 0.045$ mm, dried for 24 h) with a 40 kV generator voltage and a 30 mA current, the step size was 0.01°, and the scan range $2\theta = 10.1^\circ$ to 110° .

The percent yields of solid and liquid products were determined from the known weight of the collected products and the initial weight of the coconut shell. The gas yield was then determined from the mass balance. Table 1 summarizes the experimental conditions used to study the catalytic gasification of the coconut shell in this work.

To test the reproducibility of the experimental data, all the gasification experiments were repeated three times (triplicate tests) for each gasification condition. The standard deviation of error (σ) of solid and gas yields was estimated by the following formula: $\sigma = [\sum(x_i - \bar{x})^2 / (n - 1)]^{1/2}$, where x_i is solid yield or gas yield of sample i (no analysis was made on

TABLE 2: Proximate and ultimate analysis of coconut shell precursor.

Proximate analysis (%weight)		Ultimate analysis (%weight)	
Moisture	2.06	Hydrogen	6.52
Volatile matter	78.95 (80.61 ^{db})	Carbon	54.67
Ash	0.31 (0.32 ^{db})	Nitrogen	0.57
Fix carbon	18.68 (19.07 ^{db})	Sulphur	0.02
		Oxygen (by diff.)	38.22

^{db}Dry basis.

the gas composition), \bar{x} is arithmetic average of the triplicate test results, and n is number of product samples = $16 \times 3 = 48$ for each solid yield and gas yields.

The standard deviations of error were found to be 6.43 and 8.47 for the solid yield and gas yield, respectively. This indicates that the reproducibility of the gas yield is somewhat less than that of the solid yield. The average errors (percent deviation from mean) were estimated to be 4.95% and 6.40% for the solid yield and gas yield, respectively.

3. Results and Discussion

3.1. Raw Material Characterization. Table 2 shows the proximate and ultimate analyses of the coconut shell precursor used in this work. It is noted that the coconut shell has high content of volatile matter and low contents of ash, nitrogen, and sulfur. The precursor contains low composition of ash which is advantageous for the synthesis of highly porous activated carbons with a high yield [27]. The fixed carbon

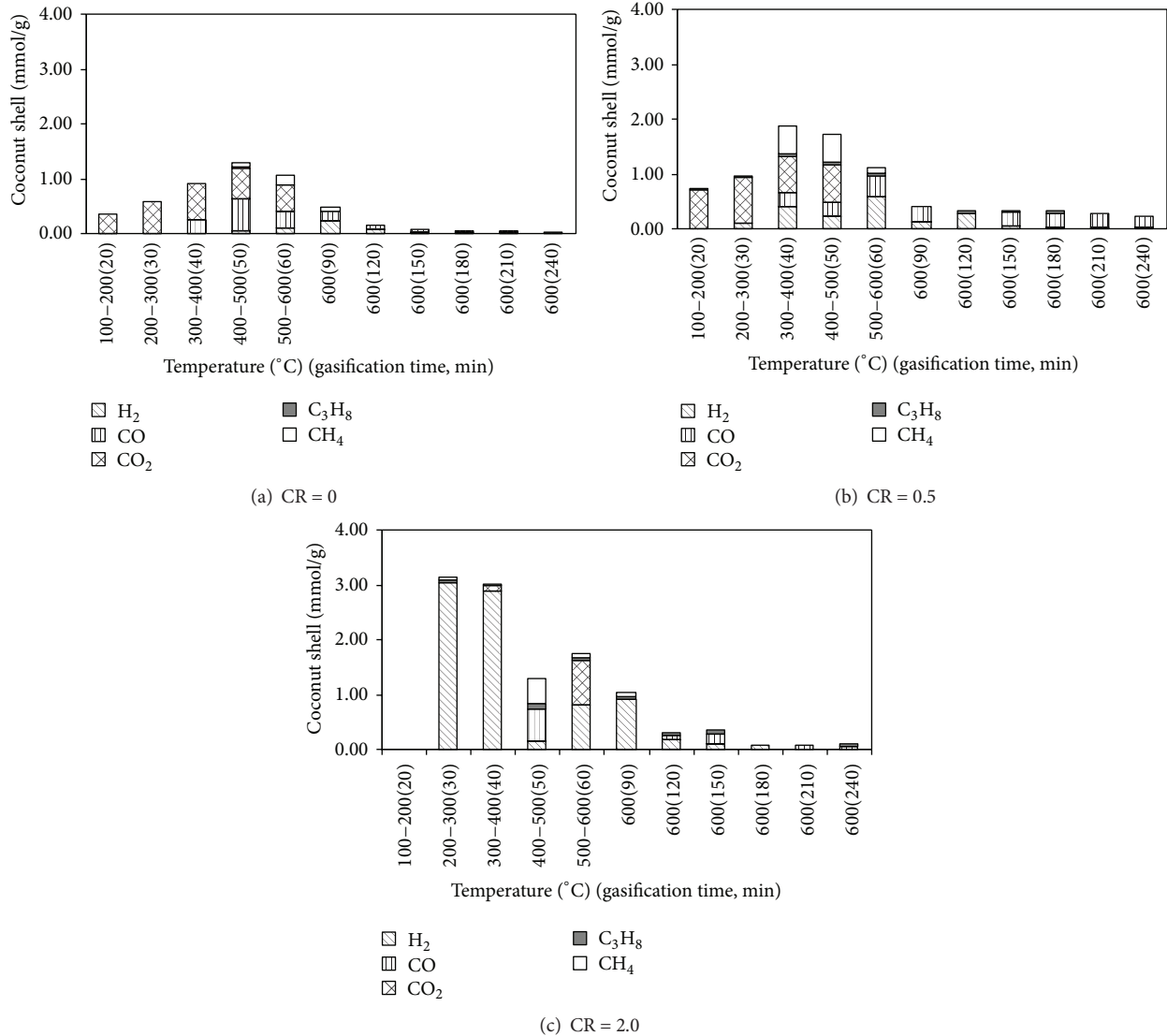
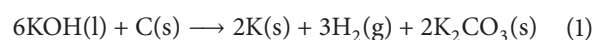


FIGURE 1: The effect of chemical weight ratio on the composition of gas products generated during the CO₂ gasification at 600°C for 180 min.

composition of 19.07% does not greatly differ from the values of 18.75% and 23.3%, as reported by Yang et al. (2010) [27] and Mohammed et al. (2015) [28], respectively. From the ultimate analysis, the carbon content of the precursor from this study (54.67%) is higher than the previously reported values of 48.7%, 48.6%, and 53.4%, respectively, by Mohammed et al. (2015) [28], Daud and Ali (2004) [29], and Demirbas (2009) [30]. It is also observed that the coconut shell contains high carbon content (>50%) which makes it suitable as a potential precursor for activated carbon production [31]. The relatively low nitrogen and sulfur contents indicate that NO_x and SO_x emissions during the gasification process should be minimal. Furthermore, the low content of sulfur decreases the possibility of acid species formation which can produce acid rain or corrode the metallic parts of gasification systems.

3.2. Properties of Syngas Product. The effect of time/temperature history on the yield and composition of produced gas

during the heat-up period from room temperature to the final gasification temperature of 600°C is shown in Figure 1. The results indicate that hydrogen gas could be generated at a lower temperature as the chemical ratio was increased. Generation of hydrogen gas started at the temperature range of 400–500°C when the gasification occurred in the absence of potassium hydroxide (Figure 1(a)) and reduced to the temperature range of 200–300°C with the addition of potassium hydroxide of chemical ratios 0.5 (Figure 1(b)) and 2.0 (Figure 1(c)). The generation of hydrogen over the low temperature range in the presence of KOH was hypothesized here to possibly occur via the reaction of KOH in the liquid state with carbon (1) [32]. In KOH/carbon system, KOH can undergo a phase transformation from solid to liquid at a temperature around 120°C or higher [32]:



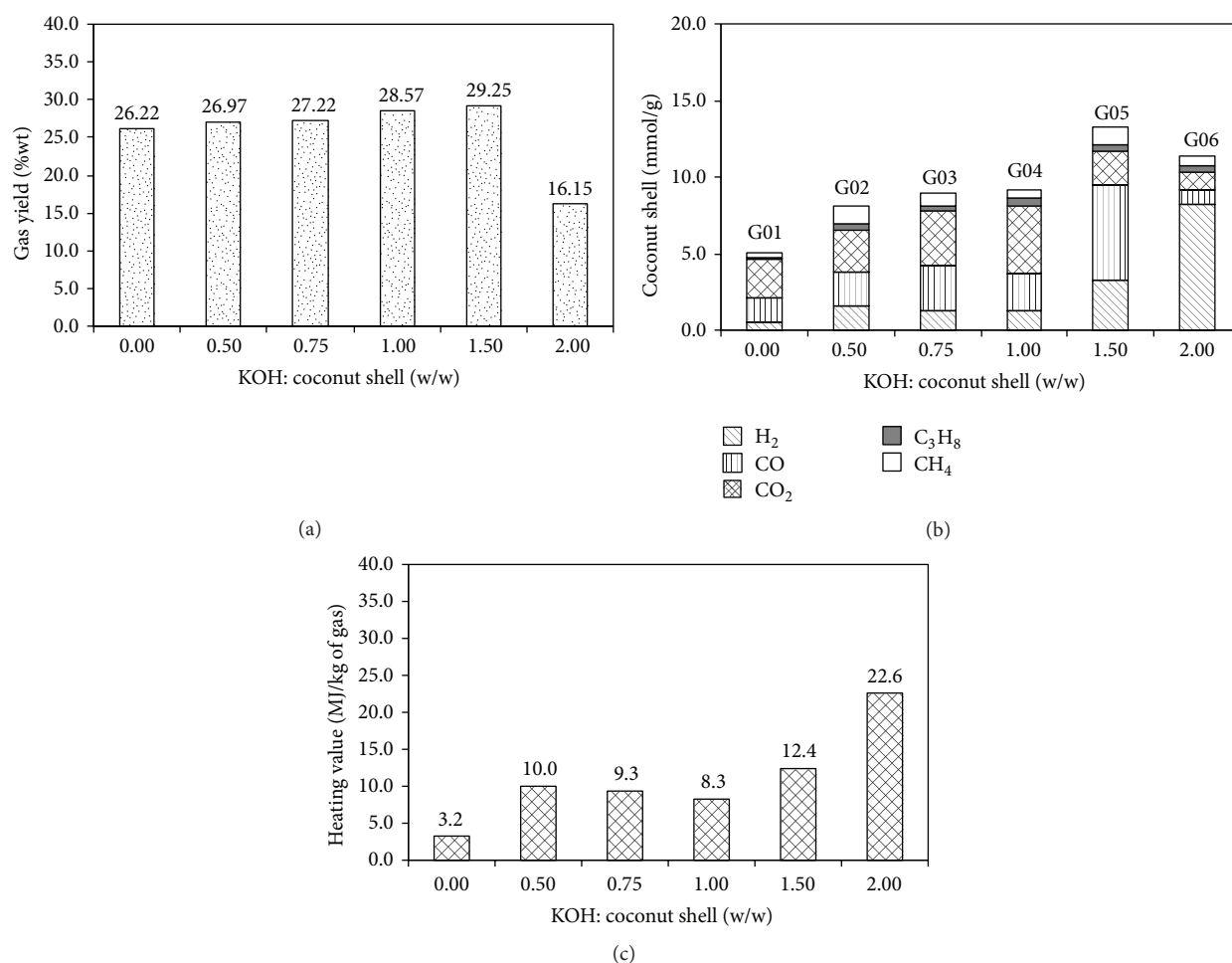


FIGURE 2: Effect of chemical weight ratio on (a) production yield, (b) composition, and (c) heating value of gas products from gasification of coconut shell with CO₂ and KOH at 600°C for 180 min.

As for the gas generation, carbon dioxide was detected in the temperature range of 200–600°C, 200–500°C, and 500–600°C when the reaction occurred without KOH and with chemical ratios of 0.5 and 2.0, respectively. The large quantities of carbon monoxide and methane were detected between 400 and 500°C when the chemical ratio of 2.0 was employed. The methane gas evolution was generated at lower temperatures when the chemical ratio was increased. In the case of the chemical ratio of 0.5, it was found that methane was generated over the 300–500°C temperature range. Figure 1 also indicates that the total amount of syngas increased with time until it reached a maximum value and then decreased. The result shows that the gasification time up to 120 min was sufficient to collect most of the generated gas sample for all chemical weight ratios. The maximum amount of gas samples was obtained between 400 and 500°C when the reaction occurred in the absence of potassium hydroxide and reduced to 300–400°C and 200–300°C when the reaction occurred with the potassium hydroxide weight ratios of 0.5 and 2.0, respectively.

The results of product gas yields, composition, and heating values under various gasification conditions are shown

in Table 3 and Figure 2. On studying the effect of chemical loading, the amount of potassium hydroxide catalyst per weight of the coconut shell was varied in the range from 0 to 2.0 g/g and the gasification was performed at 600°C for 180 min (samples G01–G06). As shown in Figure 2(a), the gas product yield increased steadily over a narrow range from 26.22% to 29.25% when the chemical weight ratio was increased from zero to 1.5 and then dropped significantly with an increasing chemical ratio from 1.50 to 2.0. On the gas composition, Figure 2(b) indicates that carbon dioxide was the main gas product accounting for 43.97 %wt for CO₂ gasification without potassium hydroxide (G01), along with some amounts of carbon monoxide (16.40 %wt), hydrogen (0.40 %wt), and methane (2.16 %wt). The composition of propane was not found in the gas products under this condition. It should be noted that the amount of carbon dioxide generated from gasification is determined by the difference between the amount of carbon dioxide detected at the exit and that fed to the reactor. Also, the total amount of detected gas products tended to increase steadily with an increasing chemical weight ratio and dropped at a chemical ratio larger than 1.5 (Figure 2(b)). The total amount of gas products was

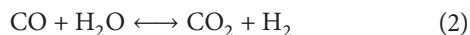
TABLE 3: Yields and composition of produced gas under various gasification conditions (see Table 1 for sample code).

Sample ID	Gas yield (%)	Gas composition (mmol/g)						Gas composition (%w)					Heating value	
		H ₂	CO	CO ₂	C ₃ H ₈	CH ₄	H ₂	CO	CO ₂	C ₃ H ₈	CH ₄	Other	MJ/kg gas	MJ/kg of coconut shell
G01	26.22	0.53	1.54	2.62	0.00	0.35	0.40	16.40	43.97	0.00	2.16	37.07	3.2	0.84
G02	26.97	1.58	2.19	2.81	0.38	1.12	1.17	22.74	45.85	6.16	6.67	17.41	10.0	2.68
G03	27.22	1.23	2.98	3.56	0.38	0.76	0.91	30.68	57.57	6.12	4.44	0.28	9.3	2.53
G04	28.57	1.25	2.43	4.38	0.57	0.49	0.81	22.06	62.42	8.15	2.56	4.00	8.3	2.38
G05	29.25	3.28	6.24	2.14	0.44	1.22	1.83	48.74	26.26	5.38	5.43	12.36	12.4	3.62
G06	16.15	8.23	0.89	1.18	0.44	0.64	10.20	15.45	32.15	11.85	6.37	23.98	22.6	3.64
G07	9.10	0.88	0.71	1.51	0.00	0.07	1.92	21.76	72.82	0.15	1.15	2.20	5.1	0.47
G08	12.55	1.03	2.43	0.78	0.01	0.03	1.65	54.24	27.36	0.18	0.38	16.19	7.7	0.97
G09	17.17	0.85	4.13	0.69	0.02	0.98	0.99	67.35	17.68	0.46	9.17	4.35	12.8	2.20
G10	17.86	1.23	2.98	3.10	0.38	0.76	0.91	30.70	50.16	6.12	4.44	7.67	9.3	1.66
G11	7.95	7.16	0.10	0.75	0.03	0.23	18.18	3.63	42.04	1.60	4.71	29.84	25.2	2.01
G12	7.46	7.49	0.10	0.96	0.03	0.20	20.29	3.80	57.44	1.48	4.25	12.74	27.5	2.05
G13	7.42	7.97	0.11	1.14	0.02	0.17	21.58	4.19	67.78	1.34	3.69	1.42	28.7	2.13
G14	7.90	8.67	0.05	0.82	0.07	0.18	22.22	1.82	45.97	3.80	3.73	22.46	30.4	2.40
G15	7.99	11.11	0.05	0.04	0.30	0.00	27.90	1.81	2.31	16.50	0.00	51.48	41.4	3.31
G16	7.82	11.73	0.06	0.00	0.10	0.29	29.23	2.03	0.00	5.39	5.75	57.60	40.6	3.17

reduced by approximately 20% when the chemical weight ratio was increased from 1.5 to 2.0. Gasification using both the potassium hydroxide and carbon dioxide appeared to promote the generation of hydrogen, carbon monoxide, and hydrocarbon gases but tended to reduce the amount of carbon dioxide generation at a chemical ratio greater than 1.0 (samples G05 and G06). Also, increasing the amount of potassium hydroxide showed an increase in the hydrogen contents in the produced gas with the chemical ratio of 2.0 (sample G06) giving the highest generated amount. It is also observed that the maximum generation of hydrogen in the produced gas was 15.5 times higher than the case without potassium hydroxide (cf. G06 versus G01).

This result could stem from the improvement of the water-gas shift reaction (2) caused by the presence of potassium hydroxide that releases more water upon heating, according to (3).

Water-gas shift reaction is as follows:



KOH decomposition is as follows:



It should be noted that the decomposition of KOH can occur over the temperature range of 400–450°C [33].

Furthermore, the increase in hydrogen content could possibly result from the dehydrogenation reaction of KOH that could occur during gasification as suggested by Viswanathan et al. (2009) [34]. Equation (4) shows such a proposed chemical pathway:



It is interesting to note from Figure 2(b) that the highest amount of carbon monoxide generated per gram of coconut

shell was evidently achieved at the chemical weight ratio of 1.5 (sample G05). Results from the gas analysis indicate that the amount of propane gas appeared to increase with increasing chemical weight ratio. However, the amount of propane gas detected is relatively small when compared with the total amount of the gas produced. The heating values of the gas products were calculated based on the measured gas composition and the heating value of the combustible gas components, including H₂, CO, CH₄, and C₃H₈. As Figure 2(c) shows, the heating value varies in the range from 3.2 to 22.6 MJ/kg of produced gas as the chemical weight ratio was increased from zero to 2.0 g/g. The highest heating value of produced gas was obtained at the chemical weight ratio of 2.0 (22.6 MJ/kg of gas), coinciding with the maximum production of hydrogen gas at this chemical weight ratio, and this result could be well explained by the role of KOH as discussed earlier.

The effect of gasification temperature on the yield, composition, and heating value of produced gas for the gasification time of 180 min and the chemical ratio of 0.75 is shown in Figure 3. The gas yield was found to increase with increasing the gasification temperature from 300 to 500°C and with a slight increase from 500 to 600°C (Figure 3(a)). The total amount of gas produced (in mmol/g coconut shell) shows a tendency of steady increase with an increasing gasification temperature, as shown in Figure 3(b). On the gas composition, carbon monoxide content increased with an increasing temperature up to the maximum of 500°C, while the amount of hydrogen produced remained relatively constant. A clear increase in the gas yields with an increasing gasification temperature could be attributed to the increased rates of devolatilization during the pyrolysis step [35], cracking reactions of the tar, and gasification reaction of the char. Also, the component of methane was found at the gasification

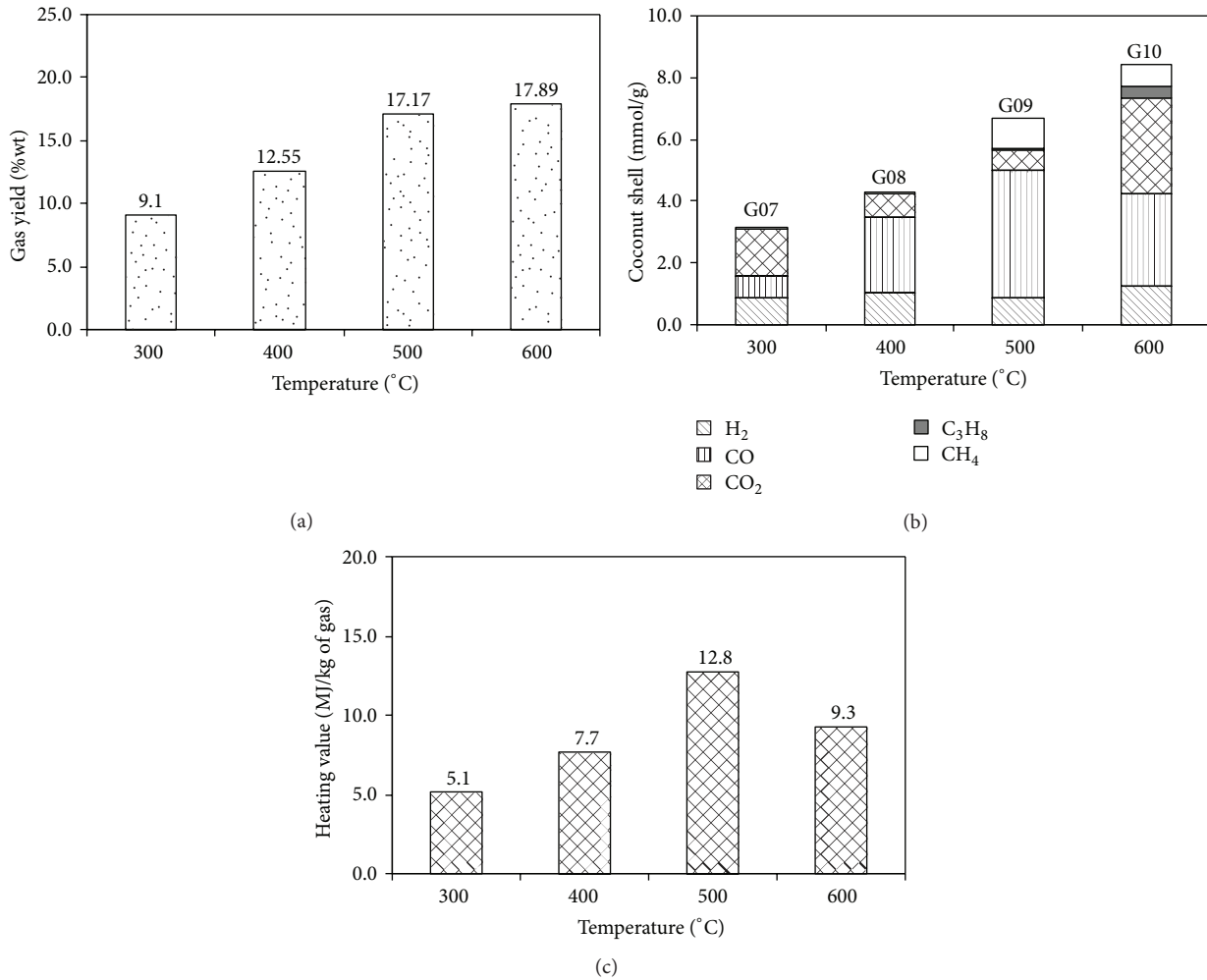


FIGURE 3: Effect of temperature on (a) gas yield, (b) composition, and (c) heating value of gas products from CO₂ gasification of coconut shell for 180 min and chemical ratio of 0.75.

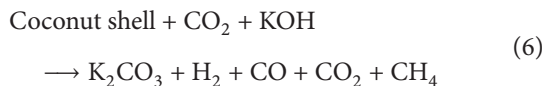
temperature of 500 °C or higher and the component of propane was detected only at the highest temperature of 600 °C (G10). Figure 3(c) shows that the heating value of the produced gas appeared to increase from 5.1 to the maximum of 12.8 MJ/kg of gas when the gasification temperature was increased from 300 to 500 °C and then drop to 9.3 MJ/kg of gas when the temperature was further increased from 500 to 600 °C. Obviously, this drop in the gas heating value should be the consequence of the decrease in carbon monoxide and the increase in carbon dioxide contents, as shown in Figure 3(b).

From these obtained results, the gasification schemes for the low temperature gasification process without a prior carbonization step could be proposed as follows:

(1) Gasification with carbon dioxide only:



(2) Gasification with both carbon dioxide and potassium hydroxide:



The possible existence of these reaction schemes is further supported by the results of XRD analysis of the final solid product before the washing step, as shown in Figure 4. The peak of K₂CO₃ compound at $2\theta \approx 32.46^\circ$ is observed on the intense line of activated carbon samples from coconut shell gasification with only potassium hydroxide (KOH) and combined potassium hydroxide and carbon dioxide (KOH + CO₂). This indicates that the formation of K₂CO₃ occurs by the reaction of KOH with CO₂ present in the gasification process.

The effect of the carbonization step on the yield, composition, and heating value of the gas products was investigated at 600 °C for 180 min and the chemical weight ratio of 2.0 and the results are shown in Figure 5. It was found that carbonization step led to a large decrease in the gas yield and this is obviously the result of excluding the amount of gas products released from the carbonization step. Figure 5(b) also shows that the main gas products from gasification of coconut shell without carbonization step (G06) were hydrogen, carbon dioxide, and carbon monoxide. However, when incorporating the carbonization step (G11) prior to the

TABLE 4: Yields and porous properties of the activated carbons from various gasification conditions (see Table 1 for details of sample code).

Sample ID	Yield (%)	Surface area (m ² /g)	Micropore volume (cm ³ /g)	Meso- and macropore volume (cm ³ /g)	Total pore volume (cm ³ /g)	Micropore volume (%)	Meso- and macropore volume (%)	Average pore diameter (nm)
G01	28.13	119	0.0633	0.0064	0.0697	90.82	9.18	2.34
G02	25.51	569	0.2544	0.0082	0.2626	96.88	3.12	1.85
G03	25.09	640	0.2950	0.0094	0.3044	96.91	3.09	2.75
G04	23.02	619	0.2839	0.0123	0.2962	95.85	4.15	1.91
G05	18.59	670	0.3267	0.0115	0.3382	96.60	3.40	2.02
G06	14.18	1000	0.4613	0.0351	0.4964	92.93	7.07	1.98
G07	31.10	*	*	*	*	—	—	—
G08	33.86	63.0	0.0519	0.0109	0.0628	82.64	17.36	3.37
G09	32.46	88.7	0.0493	0.0087	0.0580	85.00	15.00	3.25
G10	15.38	591	0.3191	0.0524	0.3715	85.90	14.10	3.12
G11	23.89	921	0.4246	0.0057	0.4303	98.68	1.32	1.87
G12	24.09	1030	0.4626	0.0105	0.4731	97.78	2.22	1.84
G13	24.97	1330	0.6014	0.0169	0.6083	98.86	1.14	1.83
G14	20.96	1710	0.7929	0.0123	0.8052	98.47	1.53	1.88
G15	20.12	2650	1.3128	0.0452	1.3580	96.67	3.33	2.05
G16	18.85	2760	1.4528	0.0321	1.4849	97.84	2.16	2.15

*Extremely low.

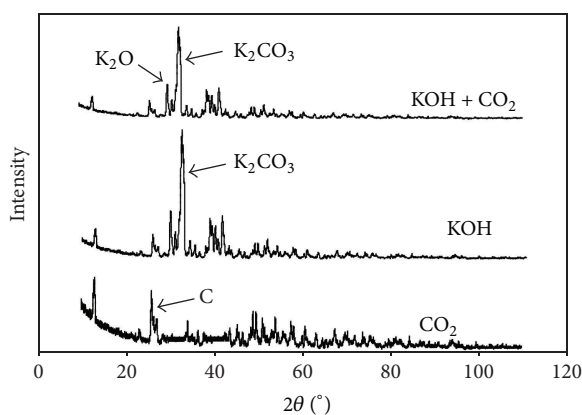


FIGURE 4: XRD patterns of activated carbons from raw coconut shell by one step gasification method (without the carbonization step) under the same conditions by using different oxidizing agents.

catalytic gasification, the main gas composition was hydrogen and carbon dioxide with hydrogen composition in %weight being much higher than the case of without carbonization (18.18 versus 10.20% as shown in Table 3). Figure 5(c) further illustrates that the incorporation of the carbonization step prior to gasification gave a slightly higher heating value of produced gas in the unit of MJ/kg gas (25.2 versus 22.6). The effect of the chemical ratio on the produced gas yield, gas composition, and gas heating value of coconut shell gasification with the carbonization step at 600°C for 60 min is shown in Figure 6. Results in Figure 6(a) indicate that the increasing of the chemical ratios did not exert a significant

effect on the gas yield. Figure 6(b) shows that the major gas composition appeared to be hydrogen followed by carbon dioxide. The amount of hydrogen and propane increased with an increasing chemical ratio from 2.0 to 4.0, while for carbon dioxide the reverse trend was observed. Figure 6(c) further shows that the heating value of the produced gas was increased from 27.5 to 41.4 MJ/kg of gas as the chemical ratio was increased from 2.0 to 4.0. This result is consistent with the corresponding increase in hydrogen content of the gas products, as illustrated in Figure 6(b).

Figures 7(a), 7(b), and 7(c) present the gas yield, gas composition, and heating value of the produced gas from coconut shell gasification with the carbonization step when the gasification temperature was varied from 600 to 700°C. It was found that the increasing of gasification temperature over this narrow range had almost no effect on the yield and heating value of the produced gas. On the other hand, it did show an influence on the gas composition. The main gas composition appeared to be hydrogen and lesser amounts of methane and propane. The composition of carbon monoxide and carbon dioxide was not found in the gas products at a gasification temperature higher than 600°C.

3.3. Porous Properties of Carbon Product. The effect of the chemical ratio on the yields and porous properties of the activated carbons produced from the coconut shell by CO₂ gasification under varying conditions is shown in Table 4 (samples G01–G16). For the gasification without the carbonization step, the chemical weight ratios between 0 and 2.0 (samples G01–G06) were tested at a fixed gasification temperature of 600°C for 180 min. It was found that the yield of solid product (activated carbon) appeared to decrease

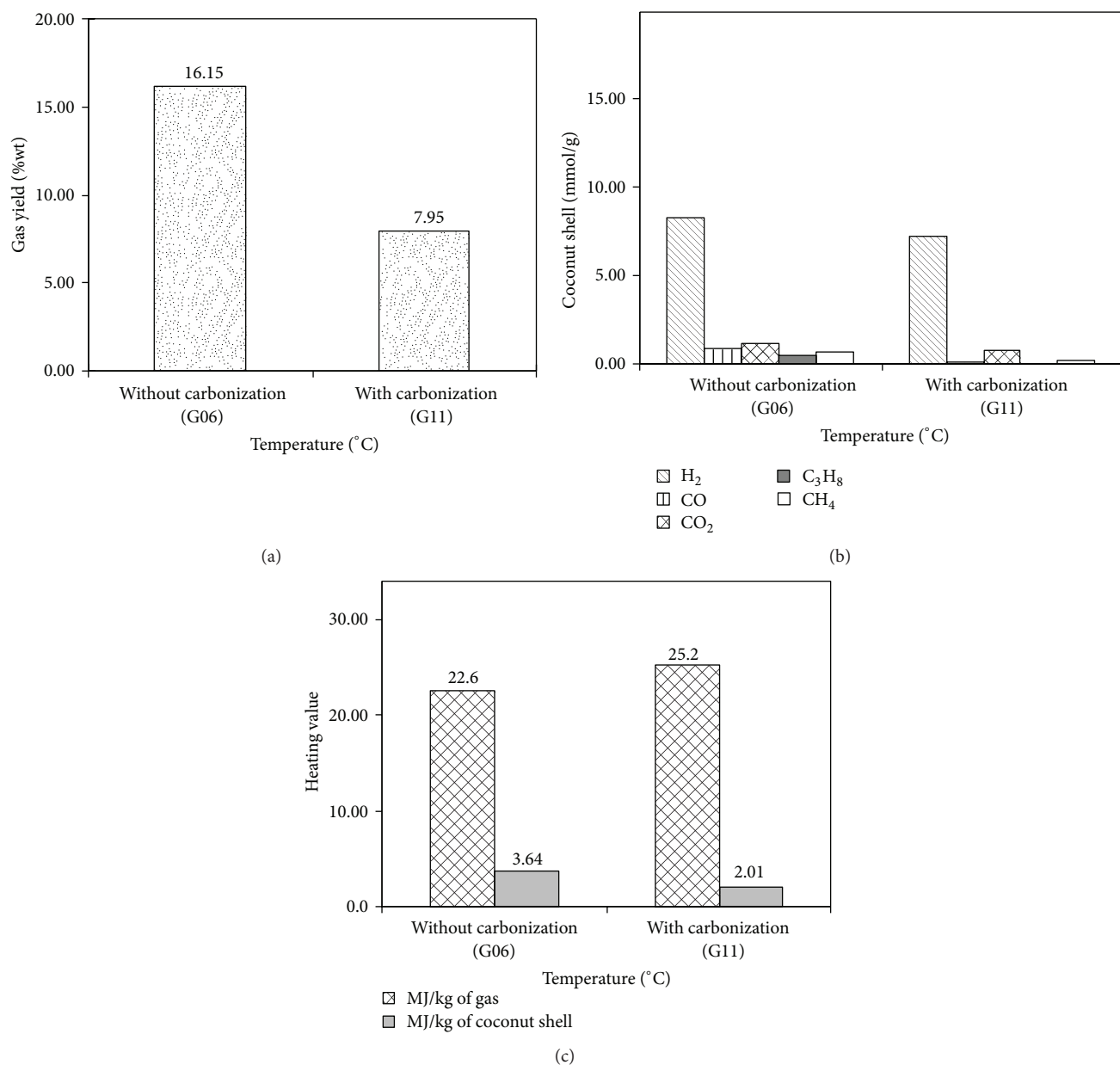


FIGURE 5: Effect of carbonization step on (a) gas yield, (b) gas composition, and (c) heating value of gas products from gasification of coconut shell with 50% CO₂ at 600°C for 180 min and chemical ratio of 2.0.

continuously from 28.13% to 14.18% when the chemical ratio was increased to the value of 2.0, as displayed in Figure 8(a). The plausible explanation to this result could be that the higher chemical weight ratio would intensify the dehydration reactions giving rise to the increasing release of volatile products [36]. KOH could also promote the gasification process because with high chemical ratio the gasification of surface carbon atoms is the predominant reaction, leading to an increase in the weight loss of the precursor [37]. Figure 8(b) shows that activated carbon from coconut shell gasification mainly consisted of micropores (more than 90%) and the average pore diameter varied in the range from 1.85 to 2.75 nm without a definite effect of the chemical ratio

(see Table 4). There is also a tendency for the mesopore and macropore volume to increase with an increasing chemical weight ratio from 0.0064 to 0.0351 cm³/g. It was also found that the specific surface area of the activated carbon product was increased by about 8.4 times (from 119 to 1000 m²/g) when gasifying with both potassium hydroxide and carbon dioxide at the maximum chemical weight ratio of 2.0 (see Figure 8(c)). The results obtained agreed with the works by Hu and Srinivasan (1999) [38] who reported that increasing the KOH chemical ratio led to a more developed porosity. There is also a tendency for the mesopores fraction of the activated carbons to increase over the chemical ratios from 1.0 to 2.0. However, the specific surface area of the solid product

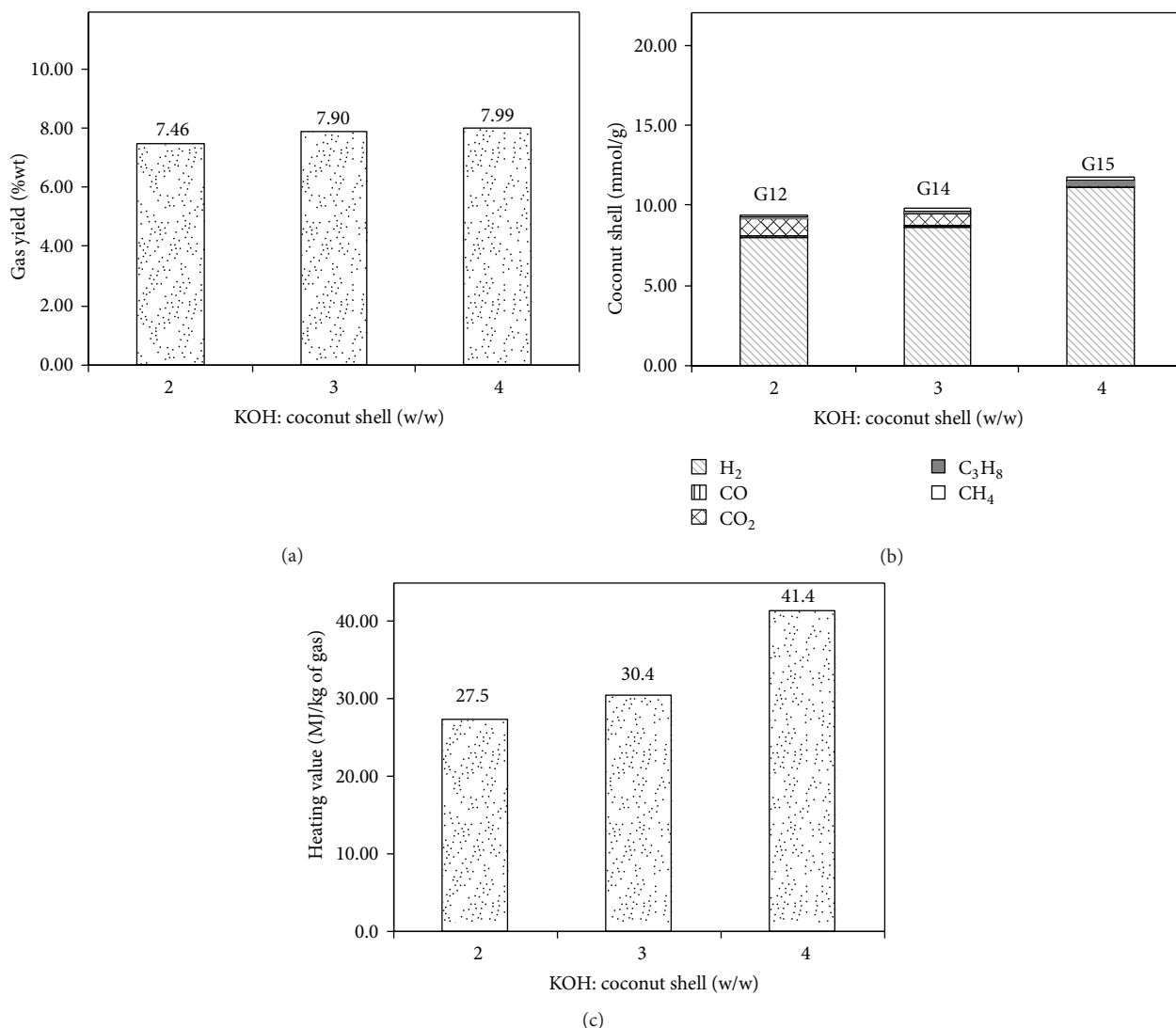


FIGURE 6: Effect of chemical ratio on gas yield and gas composition from gasification of coconut shell char with carbonization step using 50% CO₂ at 600°C for 60 min.

obtained by using only potassium hydroxide at the chemical ratio of 0.75 in the atmosphere of argon at the temperature of 600°C for 180 min (sample G10, S_{BET} of 591 m²/g) is just 8% lower than the activated carbon from the combined use of potassium hydroxide and carbon dioxide at the same chemical ratio (sample G03, S_{BET} of 640 m²/g). These results indicate that the development of porosity in activated carbon from the coconut shell at this low gasification temperature is mainly caused by the action of the chemical agent. Bansal et al. [39] have shown that the reaction between char and CO₂ is endothermic. When the activation temperature was lower than 750°C, the reaction between char and CO₂ was slow, so that the specific surface area, total pore volume, and micropore volume were relative small. Guo et al. (2009) [8] found that the maximum micropore percentage of 87.1% and 1391 m²/g of the specific surface area of the coconut shell activated carbon was obtained at the activation temperature

of 900°C using a hold time of 240 min and CO₂ flow rate of 600 cm³/min.

Table 4 indicates that at the chemical ratio of 4.0 the increase in the activation temperature from 600°C (sample G15) to 700°C (sample G16) produced a slight change in the porous properties of these samples. This indicates that above 600°C the increase in specific surface area is not significant with reference to the increased activation temperature employed.

Figure 9 presents the N₂ adsorption/desorption isotherms of an activated carbon from the coconut shell gasification using different chemical ratios of KOH (CR = 0–2) at 600°C for 180 min. All of N₂ adsorption/desorption isotherms show a similar shape, and they belong to Type I isotherm of the BDDT (Brunauer, Deming, Deming, and Teller) classification with a plateau practically parallel to the relative pressure axis and with quite a small hysteresis loop.

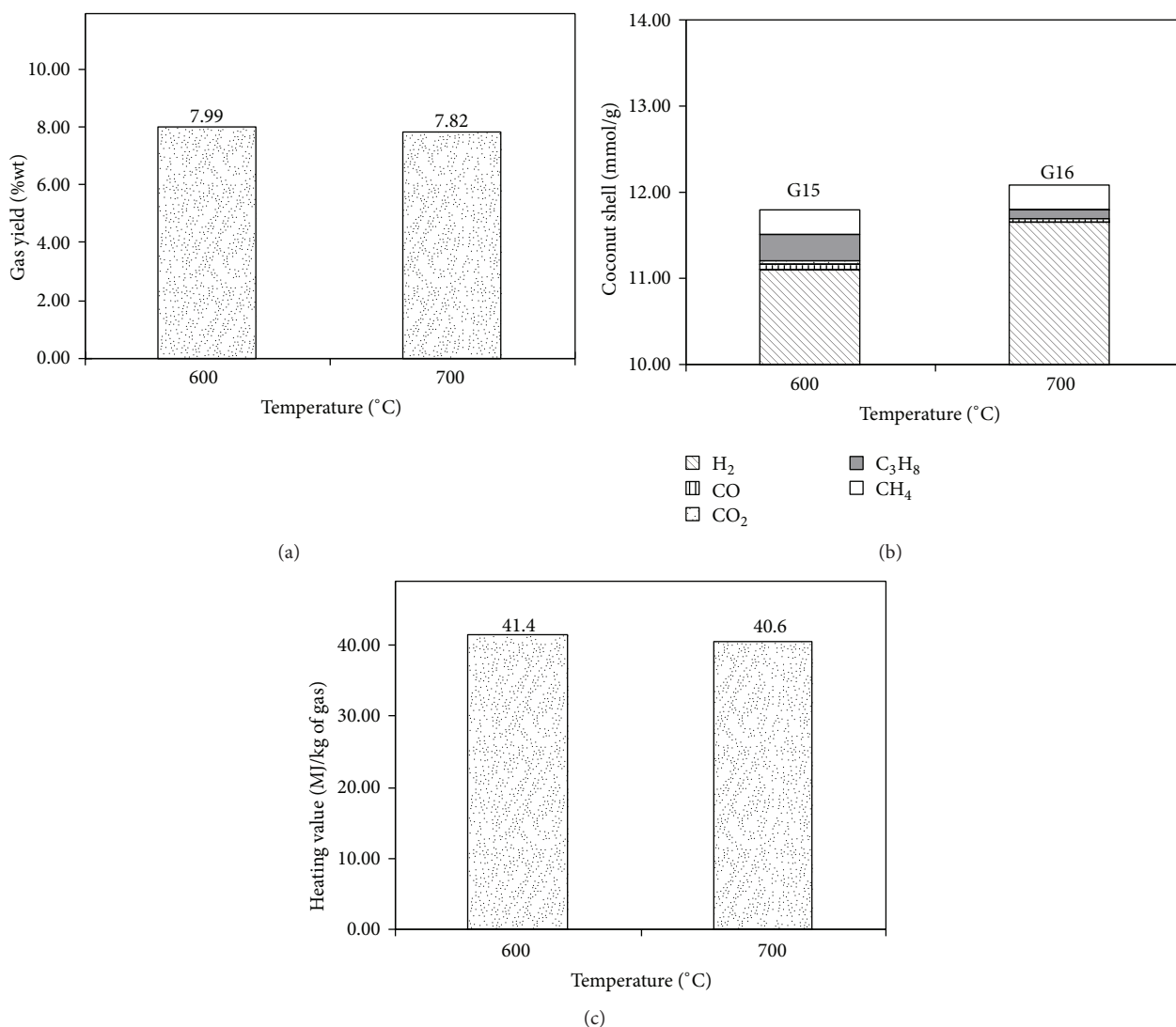


FIGURE 7: Effect of temperature on (a) gas yield, (b) gas composition, and (c) gas heating value from gasification of coconut shell with carbonization step using 50% CO₂, chemical ratio of 4.0 for 60 min.

This indicates that these carbons are essentially microporous with a very low meso- and macroporosity. These results are consistent with the pore volume distribution and average pore size shown in Figure 8(b) and Table 4.

Figure 10 demonstrates the effect of gasification temperature on the yield, pore volume distribution, and specific surface area of the activated carbons from coconut shell gasification without the carbonization step using both potassium hydroxide and carbon dioxide. It can be seen that the higher gasification temperature tended to lower the yields of activated carbons (Figure 10(a)). As seen from Figure 10(b) no micropores are developed at a relatively low gasification temperature of 300°C but an increase in micropore volume can be noticed at higher temperatures with a dramatic increase at 600°C. Also, a similar trend can be observed for the specific surface area of activated carbon products (Figure 10(c)). These results agree with the work of Iqbalidin et al. (2013) [40] who reported that the development

of porosity was achieved at an activation temperature higher than 500°C. Their activated carbons have been prepared from coconut shell by chemical activation with potassium hydroxide. Moreover, Table 4 indicates that increasing the activation temperature gave a decrease in the average pore size from 3.37 to 2.75 nm (cf. samples G07, G08, G0, and G03). The measured N₂ adsorption isotherms (not shown here) indicate that the volume of micropores was increased with an increasing gasification temperature because the increase in the adsorbed amount of N₂ and Type I isotherms is still observed even at the highest gasification temperature of 600°C.

When incorporating the carbonization step by heating the biomass in argon prior to gasification, the results showed a significant increase in the solid yield and a slight decrease in the porous properties of the activated carbon from the gasification process by using potassium hydroxide and carbon dioxide (see G06 and G11 in Table 3) at a gasification

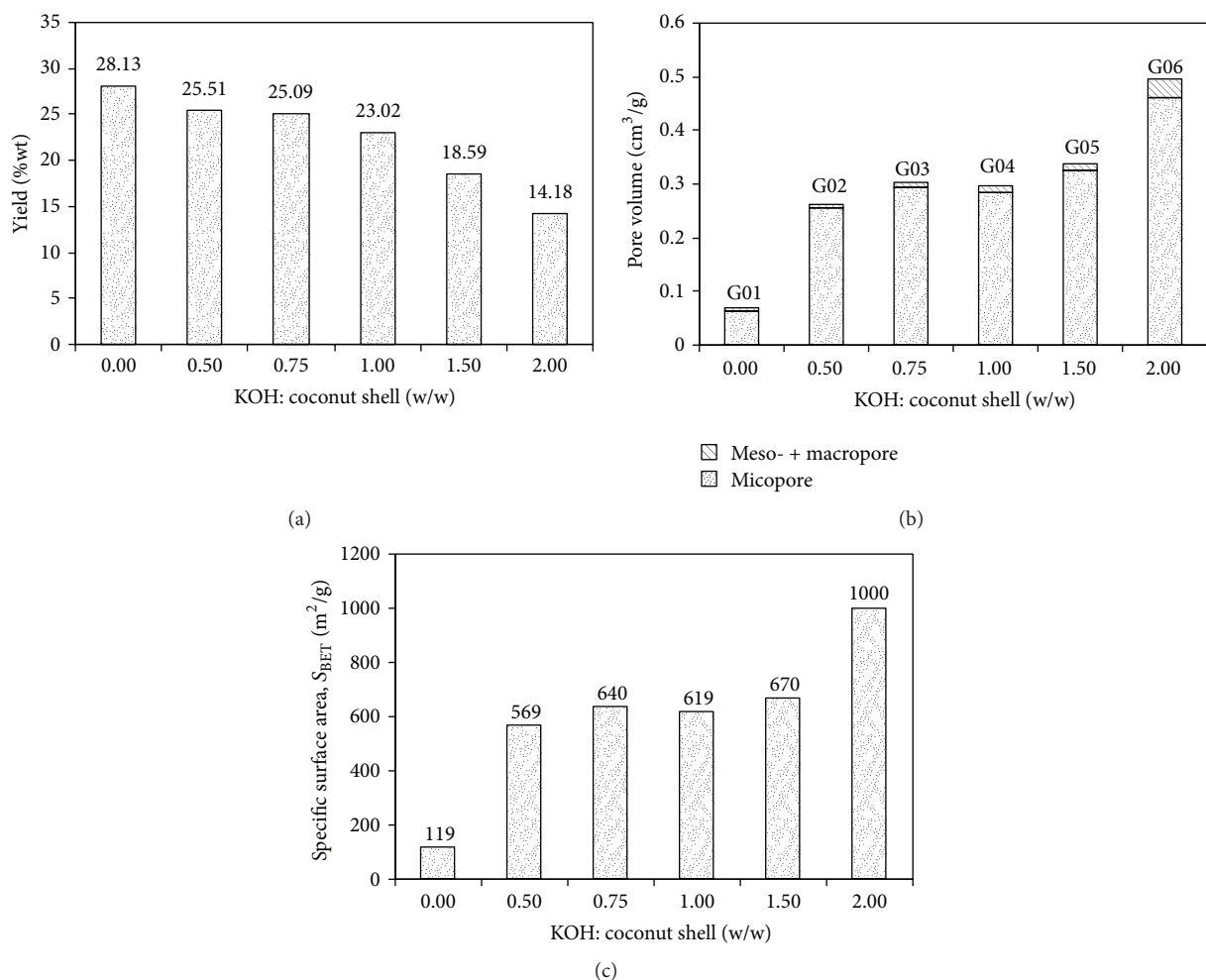


FIGURE 8: Effect of chemical ratio on (a) yield, (b) the pore volume, and (c) specific surface area (S_{BET}) of activated carbon from coconut shell gasification with potassium hydroxide and carbon dioxide at gasification temperature of 600°C for 180 min and without carbonization step.

temperature of 600°C for 180 min and chemical weight ratio of 2.0. The isotherms of G06 and G11 activated carbons show the same Type I isotherm with almost no hysteresis loop. Figure 11 indicates that the carbonization step did not strongly affect the porous properties of the activated carbon, because there are small differences in the specific surface area and pore volume. On the other hand, the incorporation of the carbonization step prior to the gasification step had an influence on the porosity properties of activated carbons when the gasification time was increased from 30 min to 180 min at a gasification temperature of 600°C (cf. G11–G13 in Table 4). The specific surface area of activated carbons was found to decrease from 1330 to 921 m²/g when the gasification time was increased from 30 to 180 min. This is probably caused by the collapse of some weak micropores at a long gasification time as is evident from the drop in the total pore volume and micropore volume. Furthermore, the experimental results show that the specific surface area of activated carbons increased by about 1.5 times when the chemical ratio was increased from 3.0 to 4.0 (cf. G14 and G15 in Table 4).

The highest surface area of activated carbons (2760 m²/g) was achievable from the gasification at a temperature of 700°C for 60 min and a chemical ratio of 4.0 with the introduced carbonization step (sample G16). This surface area is higher than that of commercial activated carbons (normally ranging from 800 to 1500 m²/g) and that reported by Geng et al. (2013) [41], who produced coconut shell activated carbon with a high surface area of 1728 m²/g by steam gasification combined with 5% HCl catalyst at 900°C.

Figure 12 summarizes the effect of gasification conditions on the specific surface area, yields of hydrogen gas and carbon monoxide gas products, and the heating value of produced gas based on the total weight of gas products and the total weight of coconut shell precursor. Figure 12(a) shows that the highest surface area of activated carbon (2760 m²/g) was obtained from the gasification at a temperature of 700°C for 60 min, at chemical ratio of 4.0, and with the carbonization step (sample G16). It was found that the carbonization step could promote the generation of hydrogen gas and appeared to inhibit the formation of carbon monoxide (Figure 12(b)). These results appear to agree with the work reported by

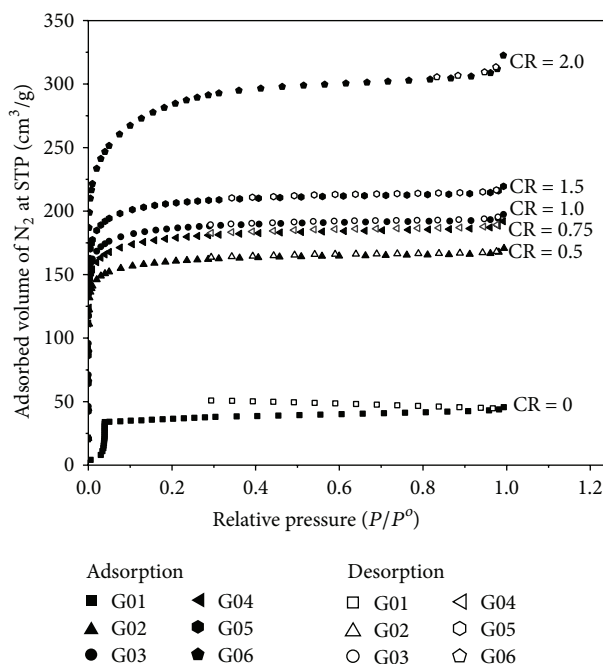


FIGURE 9: Effect of chemical ratio on nitrogen isotherm at 77 K of activated carbon samples produced by CO₂ gasification of coconut shell at 600°C for 180 min.

Raut (2014) [42] who studied the effect of torrefaction (a mild pyrolysis treatment of biomass at temperatures between 200 and 320°C) on the steam gasification of wood over the temperature range from 750 to 850°C in a bubbling fluidized-bed reactor. It was discovered that the torrefied biomass produced a higher concentration of hydrogen in the syngas product as compared to the untorrefied biomass. This favorable effect of torrefaction was attributed to such factors as the decreasing oxygen/carbon ratio, improvement of pore structure of char, and the destruction of wood fiber structure that could enhance the yield and hence the quality of the syngas product.

As shown in Figure 12(c), the maximum concentration of carbon monoxide of 67 %wt was found at the gasification without carbonization step at 500°C for 180 min and chemical ratio of 0.75 (sample G09). However, the high surface area activated carbon could not be achieved under those gasification conditions. Figure 12(d) further shows that the variation of heating value per kilogram of gas products is related to the composition of hydrogen and carbon monoxide and the results indicate that the carbonization step could enhance the heating value per kilogram of gas products. On the other hand, if the heating value is expressed based on the weight of the coconut shell, the results indicate that the carbonization step does not give an improvement on the heating value (Figure 12(e)). Finally, from the experimental results it can be inferred that the optimal condition for achieving high hydrogen composition (27.90 %wt) and propane composition (16.50 %wt) of produced gas, highest heating value (41.4 MJ/kg of gas and 3.31 MJ/kg of coconut shell), and high specific surface area (2,650 m²/g) of produced activated carbon is to employ the gasification temperature

of 600°C for 60 min and chemical ratio of 4.0 with the incorporation of carbonization step (sample G15).

4. Conclusions

An attempt was made to investigate the CO₂ gasification of coconut shell biomass at low temperatures from 300 to 700°C using KOH as a catalyst. Increasing catalyst loading and temperature had a favorable effect on promoting the porous properties of activated carbon product. The incorporation of the carbonization step prior to gasification slightly decreases surface area and pore volume of resulting carbon products. Catalyst loading and gasifying temperature showed a significant influence on the yield, composition, and heating value of the syngas product. Carbon dioxide was found to be the main gas component for CO₂ gasification without KOH. However, gasifying the coconut shell with both CO₂ and KOH could enhance the generation of hydrogen and carbon monoxide and retard the formation of carbon dioxide. The heating value of gas products tended to increase with the amount of KOH catalyst and to increase with temperature in the range from 300 to 500°C. Gas yield decreased substantially when the carbonization step was included prior to gasification but the gas heating value was not greatly affected. The optimal condition for achieving high hydrogen composition (27.90 %weight), high heating value (41.4 MJ/kg of gas) of produced gas, and high specific surface area (2650 m²/g) of activated carbon product was to first carbonize coconut shell and gasify the resultant char at 600°C for 60 min using chemical weight ratio of 3.0. Finally, it might be worthwhile to continue this work on analyzing the economic feasibility of this low

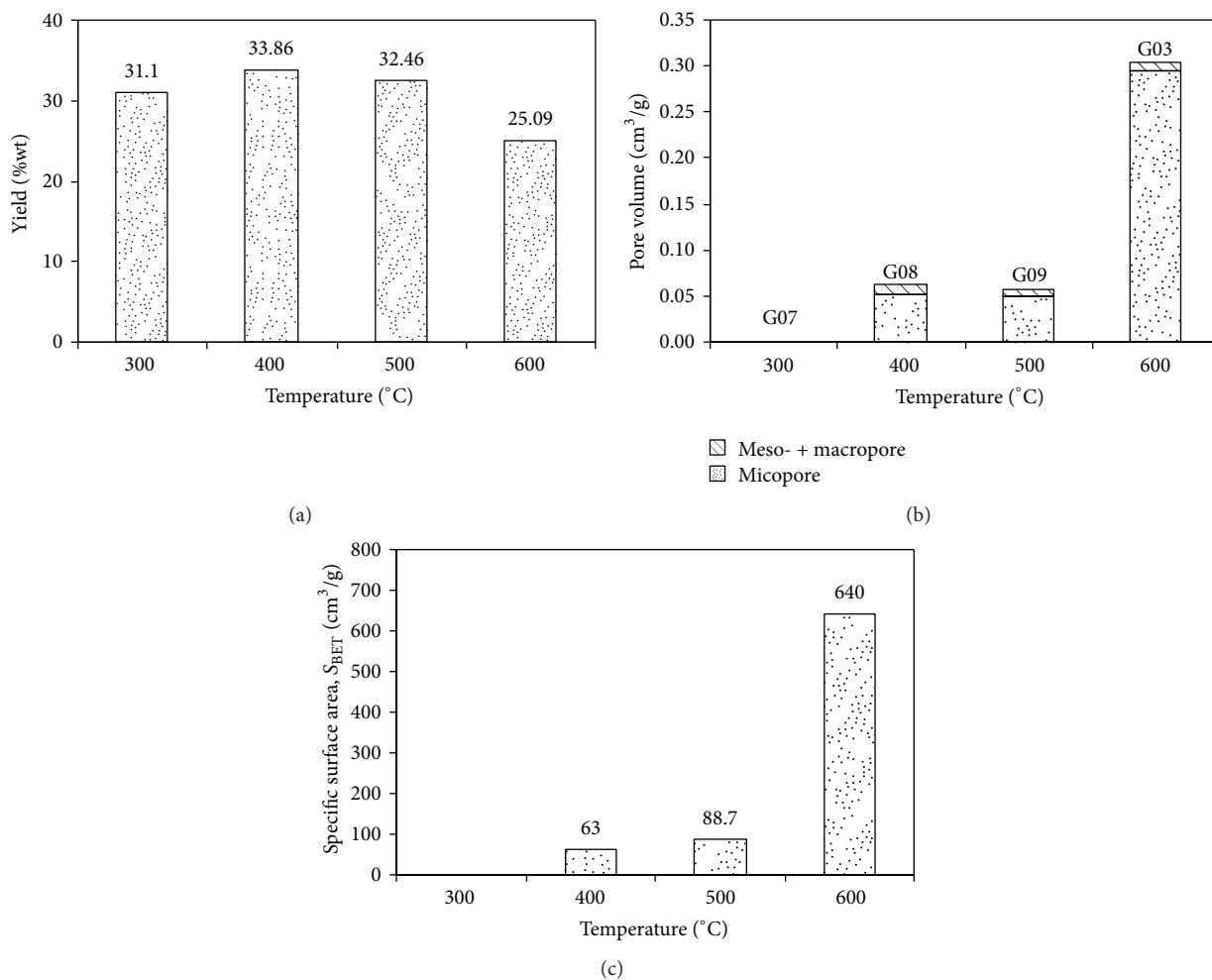


FIGURE 10: Effect of gasification temperature on (a) yield, (b) pore volume, and (c) specific surface area (S_{BET}) of activated carbon from coconut shell with the combined use of potassium hydroxide and carbon dioxide at chemical ratio of 0.75, 180 min, and without carbonization step.

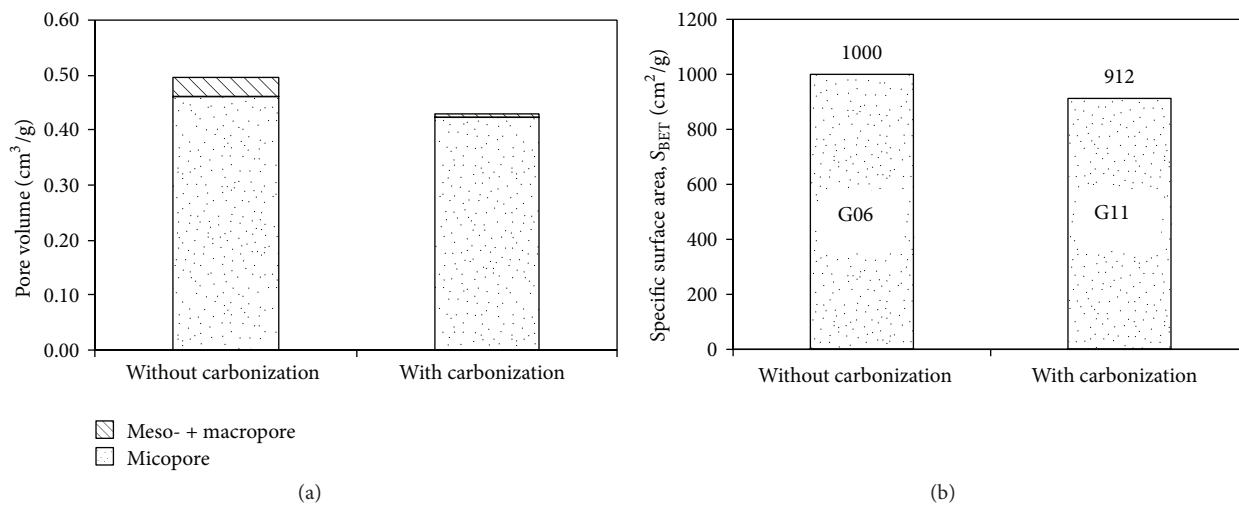


FIGURE 11: Effect of carbonization step on (a) pore volume and (b) specific surface area (S_{BET}) of activated carbon from coconut shell by gasification with potassium hydroxide and carbon dioxide at 600°C for 180 min and chemical ratio of 2.0.

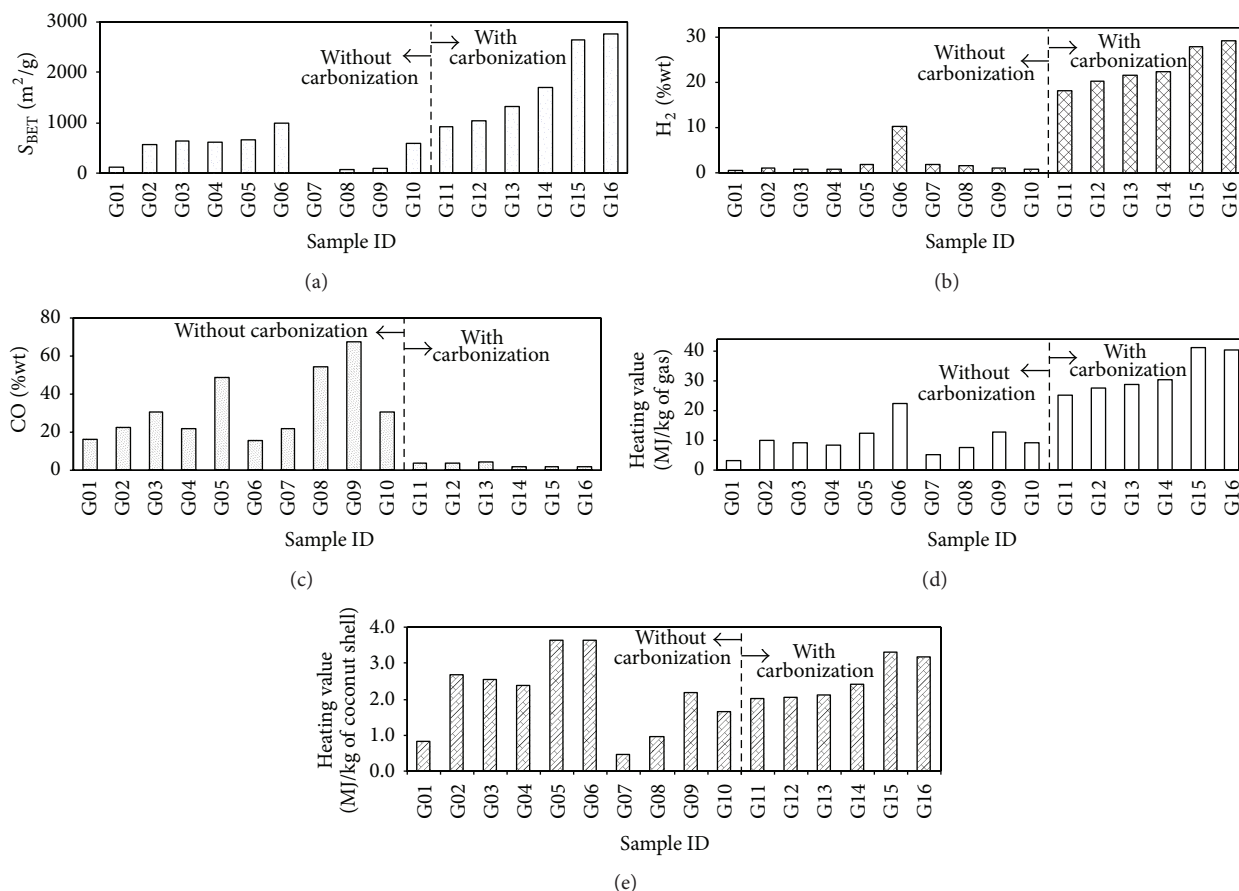


FIGURE 12: Effect of gasification conditions on (a) specific surface area, (b) hydrogen gas yield, (c) carbon monoxide gas yield, (d) heating value of gas, and (e) heating value of gas base on weight of coconut shell precursor.

temperature catalytic gasification of biomass for large-scale applications.

Conflict of Interests

The authors declare that there is no conflict of interests regarding the publication of this paper.

Acknowledgments

This research was financially supported by The Ministry of Science and Technology of Thailand and The Advanced Low Carbon Technology Research and Development Program (ALCA) funded by Japan Science and Technology Agency.

References

- [1] P. Basu, *Biomass Gasification and Pyrolysis: Practical Design and Theory*, Elsevier, London, UK, 2010.
- [2] M. Crocker, *Thermochemical Conversion of Biomass to Liquid Fuels and Chemicals*, vol. 7, Royal Society of Chemistry, London, UK, 2010.
- [3] K. S. Lin, H. P. Wang, C.-J. Lin, and C.-I. Juch, "A process development for gasification of rice husk," *Fuel Processing Technology*, vol. 55, no. 3, pp. 185–192, 1998.
- [4] T. Hosoya, H. Kawamoto, and S. Saka, "Cellulose-hemicellulose and cellulose-lignin interactions in wood pyrolysis at gasification temperature," *Journal of Analytical and Applied Pyrolysis*, vol. 80, no. 1, pp. 118–125, 2007.
- [5] R. Yin, R. Liu, J. Wu, X. Wu, C. Sun, and C. Wu, "Influence of particle size on performance of a pilot-scale fixed-bed gasification system," *Bioresource Technology*, vol. 119, pp. 15–21, 2012.
- [6] X. L. Yin, C. Z. Wu, S. P. Zheng, and Y. Chen, "Design and operation of a CFB gasification and power generation system for rice husk," *Biomass and Bioenergy*, vol. 23, no. 3, pp. 181–187, 2002.
- [7] P. A. Salam and S. C. Bhattacharya, "A comparative study of charcoal gasification in two types of spouted bed reactors," *Energy*, vol. 31, no. 2-3, pp. 228–243, 2006.
- [8] S. Guo, J. Peng, W. Li et al., "Effects of CO_2 activation on porous structures of coconut shell-based activated carbons," *Applied Surface Science*, vol. 255, no. 20, pp. 8443–8449, 2009.
- [9] L. García, M. L. Salvador, J. Arauzo, and R. Bilbao, "Catalytic steam gasification of pine sawdust. Effect of catalyst weight/biomass flow rate and steam/biomass ratios on gas production and composition," *Energy and Fuels*, vol. 13, no. 4, pp. 851–859, 1999.
- [10] L. Meng, M. Wang, H. Yang, Y. Hongyan, and L. Chang, "Catalytic effect of alkali carbonates on CO_2 gasification of

- Pingshuo coal,” *Mining Science and Technology*, vol. 21, no. 4, pp. 587–590, 2009.
- [11] A. Sharma, I. Saito, H. Nakagawa, and K. Miura, “Effect of carbonization temperature on the nickel crystallite size of a Ni/C catalyst for catalytic hydrothermal gasification of organic compounds,” *Fuel*, vol. 86, no. 7–8, pp. 915–920, 2007.
- [12] V. R. Choudhary, S. Banerjee, and A. M. Rajput, “Hydrogen from step—wise steam reforming of methane over Ni/ZrO₂: factors affecting catalytic methane decomposition and gasification by steam of carbon formed on the catalyst,” *Applied Catalysis A: General*, vol. 234, no. 1–2, pp. 259–270, 2002.
- [13] L. J. Figueiredo and J. A. Moulijn, “Carbon and coal gasification science and technology,” in *Proceedings of the NATO Advanced Study Institute on Carbon and Coal Gasification*, Science and Technology, p. 314, Alvor, Portugal, May 1985.
- [14] K. Mitsuoka, S. Hayashi, H. Amano, K. Kayahara, E. Sasaoaka, and Md. A. Uddin, “Gasification of woody biomass char with CO₂: the catalytic effects of K and Ca species on char gasification reactivity,” *Fuel Processing Technology*, vol. 92, no. 1, pp. 26–31, 2011.
- [15] S. Rapagná, N. Jand, and P. U. Foscolo, “Catalytic gasification of biomass to produce hydrogen rich gas,” *International Journal of Hydrogen Energy*, vol. 23, no. 7, pp. 551–557, 1998.
- [16] P. Chairprasert and T. Vitidsant, “Promotion of coconut shell gasification by steam reforming on nickel-dolomite,” *American Journal of Applied Sciences*, vol. 6, no. 2, pp. 332–336, 2009.
- [17] A. Kruse, D. Meier, P. Rimbrecht, and M. Schacht, “Gasification of pyrocatechol in supercritical water in the presence of potassium hydroxide,” *Industrial and Engineering Chemistry Research*, vol. 39, no. 12, pp. 4842–4848, 2000.
- [18] J. Díaz-Terán, D. M. Nevskaja, J. L. G. Fierro, A. J. López-Peinado, and A. Jerez, “Study of chemical activation process of a lignocellulosic material with KOH by XPS and XRD,” *Microporous and Mesoporous Materials*, vol. 60, no. 1–3, pp. 173–181, 2003.
- [19] Y. Huang, X. Yin, C. Wu et al., “Effects of metal catalysts on CO₂ gasification reactivity of biomass char,” *Biotechnology Advances*, vol. 27, no. 5, pp. 568–572, 2009.
- [20] X. Wang, F. Chen, B. Hong, H. Liu, G. Yu, and F. Wang, “The steam gasification of coal catalyzed by KOH for the production of hydrogen,” *Energy Sources*, vol. 35, no. 17, pp. 1583–1589, 2013.
- [21] S. E. Abechi, C. E. Gimba, A. Uzairu, and Y. A. Dallatu, “Preparation and characterization of activated carbon from palm kernel shell by chemical activation,” *Research Journal of Chemical Sciences*, vol. 3, no. 7, pp. 54–61, 2013.
- [22] Y. Gao, Q. Yue, B. Gao et al., “Preparation of high surface area-activated carbon from lignin of papermaking black liquor by KOH activation for Ni(II) adsorption,” *Chemical Engineering Journal*, vol. 217, pp. 345–353, 2013.
- [23] G. Lota, T. A. Centeno, E. Frackowiak, and F. Stoeckli, “Improvement of the structural and chemical properties of a commercial activated carbon for its application in electrochemical capacitors,” *Electrochimica Acta*, vol. 53, no. 5, pp. 2210–2216, 2008.
- [24] Y. Xiao, C. Long, M.-T. Zheng et al., “High-capacity porous carbons prepared by KOH activation of activated carbon for supercapacitors,” *Chinese Chemical Letters*, vol. 25, no. 6, pp. 865–868, 2014.
- [25] N. Ferrera-Lorenzo, E. Fuente, I. Suárez-Ruiz, and B. Ruiz, “KOH activated carbon from conventional and microwave heating system of a macroalgae waste from the Agar-Agar industry,” *Fuel Processing Technology*, vol. 121, pp. 25–31, 2014.
- [26] D. D. Do, *Adsorption Analysis: Equilibrium and Kinetics*, Imperial College Press, London, UK, 1998.
- [27] K. Yang, J. Peng, C. Srinivasakannan, L. Zhang, H. Xia, and X. Duan, “Preparation of high surface area activated carbon from coconut shells using microwave heating,” *Bioresource Technology*, vol. 101, no. 15, pp. 6163–6169, 2010.
- [28] J. Mohammed, N. S. Nasri, M. A. A. Zaini, U. D. Hamza, and F. N. Ani, “Adsorption of benzene and toluene onto KOH activated coconut shell based carbon treated with NH₃,” *International Biodeterioration & Biodegradation*, vol. 102, pp. 245–255, 2015.
- [29] W. M. A. W. Daud and W. S. W. Ali, “Comparison on pore development of activated carbon produced from palm shell and coconut shell,” *Bioresource Technology*, vol. 93, no. 1, pp. 63–69, 2004.
- [30] A. Demirbas, *Biofuels*, Springer, London, UK, 2009.
- [31] J. N. Terasa, *Activated Carbon Surfaces in Environmental Remediation*, Interface Science and Technology, Elsevier, London, UK, 2006.
- [32] Corning Incorporate, “Chemical activation of carbon via an entrained stream method,” U. S patent no. WO2014134000 A1, 2014.
- [33] J. P. Hirtz, C. Whitehous, H. P. Meier, H. J. von Bardeleben, and M. O. Manasreh, *Semiconductor Materials for Optoelectronics and LTMBE Materials*, Elsevier Science, Amsterdam, The Netherlands, 1993.
- [34] B. Viswanathan, P. Indranee, and T. K. Varadarajan, *Methods of Activation and Specific Applications of Carbon Materials*, National Centre for Catalysis Research, Chennai, India, 2009.
- [35] K. Raveendran, A. Ganesh, and K. C. Khilar, “Pyrolysis characteristics of biomass and biomass components,” *Fuel*, vol. 75, no. 8, pp. 987–998, 1996.
- [36] D. Adinata, W. M. A. W. Daud, and M. K. Aroua, “Preparation and characterization of activated carbon from palm shell by chemical activation with K₂CO₃,” *Bioresource Technology*, vol. 98, no. 1, pp. 145–149, 2007.
- [37] Y. Sudaryanto, S. B. Hartono, W. Irawaty, H. Hindarso, and S. Ismadji, “High surface area activated carbon prepared from cassava peel by chemical activation,” *Bioresource Technology*, vol. 97, no. 5, pp. 734–739, 2006.
- [38] Z. Hu and M. P. Srinivasan, “Preparation of high-surface-area activated carbons from coconut shell,” *Microporous and Mesoporous Materials*, vol. 27, no. 1, pp. 11–18, 1999.
- [39] R. C. Bansal, J. B. Donnet, and F. Stoeckli, *Active Carbon*, Marcel Dekker, New York, NY, USA, 1988.
- [40] M. N. M. Iqbalidin, I. Khudzir, M. I. M. Azlan, A. G. Zaidi, B. Surani, and Z. Zubri, “Properties of coconut shell activated carbon,” *Journal of Tropical Forest Science*, vol. 25, no. 4, pp. 497–503, 2013.
- [41] X. Geng, L. Li, M. Zhang, B. An, and X. Zhu, “Influence of reactivation on the electrochemical performances of activated carbon based on coconut shell,” *Journal of Environmental Sciences*, vol. 25, supplement 1, pp. S110–S117, 2013.
- [42] M. K. Raut, *Studies into the effect of torrefaction on gasification of biomass [M.S. thesis]*, Dalhousie University, Nova Scotia, Canada, 2014, <http://dalspace.library.dal.ca/xmlui/handle/10222/50378>.



Hindawi

Submit your manuscripts at
<http://www.hindawi.com>

